Suppression of the Shastry-Sutherland phase driven by electronic concentration reduction in magnetically frustrated $Ce_{2.15}Pd_{1.95}(Sn_{1-y}In_y)_{0.9}$ alloys

J. G. Sereni,[1] J. Roberts,[2] F. Gastaldo,[2] and M. Giovannini[2]
[1]*Low Temperature Division, CAB-CNEA, CONICET, 8400 San Carlos de Bariloche, Argentina*
[2]*Dipartimento di Chimica, Universita' di Genova, Via Dodecaneso 33, I-16146 Genova, Italy*

(Received 17 February 2019; revised manuscript received 15 June 2019; published 14 August 2019)

Exploiting the possibility to switch from antiferromagnetic (AFM) and ferromagnetic (FM) ground states (GSs) in out-stoichiometric branches of Ce_2Pd_2In alloys, the stability of Shastry-Sutherland (ShSu) phase of Ce_2Pd_2Sn as a function of Sn/In electron doping was studied. Magnetic and specific-heat measurements show that the Ce-rich compositions stabilize the FM-GS throughout the Sn/In-FM substitution, allowing to extend the formation of the ShSu phase up to its collapse in a tricritical point around $y_{cr} = 0.5$. On the other hand, this behavior is quite different from that reported in a recent investigation on the AFM branch where atomic disorder at intermediate Sn/In-AFM concentrations inhibits the formation of the ShSu phase.

DOI: 10.1103/PhysRevB.100.054421

I. INTRODUCTION

Intermetallic compounds with the formula R_2T_2X (where $R =$ rare earths, $T =$ transition metals, and $X =$ Sn, In, Pb, or Cd) [1] have received special attention in the case of $R =$ Ce and Yb due to their varied behaviors, such as intermediate valence [2], non-Fermi liquid [3,4], and quantum phase transitions [4,5]. Most of these compounds crystallize in the tetragonal Mo_2FeB_2 type [6], whereas a few of them are formed in a related variant of U_2Pt_2Sn type. Both structures consist of alternate R planes and T, X planes stacked along the c axis. In the $z = 1/2$ layers, magnetic R atoms form a network of triangles and squares (mimicking a pinwheel mosaic) as depicted in Fig. 1. Triangular coordination between magnetic nearest-neighbors (*nn*) provides the ideal conditions for magnetic frustration and the eventual formation of a Shastry-Sutherland (ShSu) magnetic lattice as an alternative ground state, provided that *nn* interaction induces the formation of magnetic dimers, see the red dashed arrows in Fig. 1. The Euclidean distribution of interacting dimers on the $z = 1/2$ plane corresponds to a 2D network of simple squares. The physical behavior of these peculiar magnetic lattices was modeled by Shastry and Sutherland [7] and clearly realized in the covalent compound $SrCu_2(BO_3)_2$ [8]. Later, this behavior was also detected in intermetallic compounds, such as Yb_2Pt_2Pb [9,10], crystallizing in the U_2Pt_2Sn type and Ce_2Pd_2Sn [11] with the Mo_2FeB_2 type.

In the case of Ce_2Pd_2Sn, the evidence for ShSu magnetic arrangement was observed between $T_S = 4.8$ and $T_C = 2.1$ K [11]. At T_S, the Ce-Ce *nn* interaction forms ferromagnetic dimers located at the corners of the simple square lattice described in Fig. 1 as the center of the red arrows. The peculiar magnetic phase arising between these two boundaries is recognized as a ShSu phase, provided that the corresponding square lattice (or ShSu lattice) of dimers builds up. This magnetic structure become unstable once interplane interactions transform the system into a three-dimensional (3D) magnet at $T_C = 2.1$ K.

The magnetic stability of this exotic phase in Ce_2Pd_2Sn was studied under a magnetic field [12], detecting that it is suppressed at a critical field $B_{cr} = 1100 \pm 100$ Oe.

In order to test the stability of the ShSu phase as a function of electronic concentration, the progressive substitution of $[5s^25p^1]$-In atoms in the $[5s^25p^2]$-Sn lattice was recently investigated [13]. The isotypic Ce_2Pd_2In is known to form in the same Mo_2FeB_2-type structure [6] not in stoichiometric composition but as a double-branch solid solution around its stoichiometric composition [14].

The low-temperature magnetic properties of this solid solution were recognized to depend on the relative excess of Ce or Pd components, resulting in respective ferromagnetic (FM) or antiferromagnetic (AFM) ground states (GS) [14,15]. These two distinct magnetic branches allow to study the ShSu phase stability in $Ce_2Pd_2(Sn, In)$ out-stoichiometric alloys following comparable trails, one related to a FM, and the other related to an AFM-GS at the In-rich limit.

Recently [13] the Pd-rich branch, i.e., starting from the AFM state in $Ce_{1.9}Pd_{2.3}(In_{1-x}Sn_x)_{0.8}$, was reported to show relevant atomic disorder for $x \geqslant 0.4$ that inhibits the formation of the ShSu phase at higher Sn content. Probably, the excess of Pd perturbs the Ce-magnetic lattice inducing magnetic disorder. Such magnetic disorder is reflected as a broadening of the $T_N(x)$ transition at $x = 0.4$.

In this paper, we report on the stability of the ShSu phase following the FM Ce-rich branch: $Ce_{2.15}Pd_{1.95}(Sn_{1-y}In_y)_{0.9}$ that forms all along the Sn/In(y) composition and show well-defined magnetic transitions. Note that, for clarity reasons, Sn(x) concentration of the AFM case was replaced by In(y) for the FM one.

II. EXPERIMENTAL DETAILS AND RESULTS

A. Sample preparation and characterization

A series of polycrystalline samples with nominal composition $Ce_{2.15}Pd_{1.95}(Sn_{1-y}In_y)_{0.9}$ with $y = 0.2, 0.4, 0.5, 0.6, 0.8$

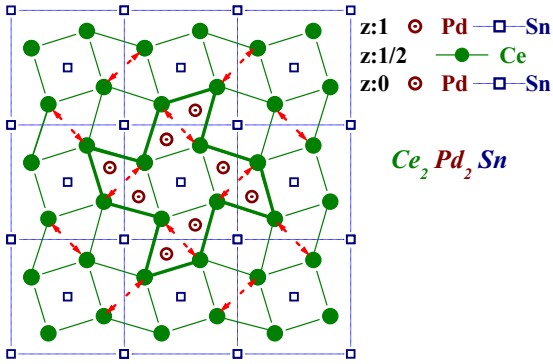

FIG. 1. Ce magnetic atoms form a network of triangles and squares (green segments) mimicking a pinwheel mosaic remarked at the center of the figure. Magnetic interaction between Ce-Ce *nn* (red arrows) form magnetic dimers, whereas interdimers interactions build up a simple two-dimensional (2D) cubic lattice [11].

were prepared by weighing the proper amounts of elements, then arc-melted in an argon atmosphere on a water-cooled copper hearth with a tungsten electrode. To ensure good homogeneity, the buttons were turned over and remelted several times. Weight losses after melting were always smaller than 0.5 mass %. Later, the samples were annealed at 750 °C for ten days and quenched in cold water. Scanning electron microscopy (SEM) and electron probe microanalysis (EPMA) based on energy-dispersive x-ray spectroscopy were used to examine phase compositions. The composition contrast was revealed in unetched samples by means of a backscattered electron detector. X-ray diffraction (XRD) was performed on powder samples using a vertical diffractometer X-Pert with Cu K_α radiation.

Rietveld refinement of powder XRD data indicates that all samples crystallize in the Mo_2FeB_2-type structure in the whole composition range. XRD data combined with SEM/EMPA data revealed, in all samples, the presence of less than 5% of Ce-oxide impurity (with T_N at 6.3 K) which was irrelevant for magnetic and thermal measurements. From EMPA, data phase compositions resulted to be coincident with synthesis compositions within standard EPMA errors of 1%. Lattice parameters slightly change along the concentration range from $a = 7.765$ to $c = 3.902$ Å with a $c/a = 0.5026$ ratio of the $x = 0$ mother compound [11].

DC-magnetization measurements were carried out using a standard superconducting quantum interference device magnetometer operating between 1.8 and 320 K and as a function of field up to 5 T. Specific heat was measured using a standard heat pulse technique in a semiadiabatic ^{3}He calorimeter in the range between 0.5 and 20 K at zero applied magnetic field.

B. Magnetic properties

High-temperature ($T >$ 30-K) magnetic susceptibility results are properly described by a $\chi = \chi_{cw} + \chi_P$ dependence, see Fig. 2(a) where the first term corresponds to the temperature-dependent Curie-Weiss contribution $\chi_{cw} = \frac{Cc}{T+\theta_P}$ and the second corresponds to a Pauli-like contribution. A weak χ_P contribution is observed along the full concentration range with values ranging within $\chi_P = (0.6 \pm 0.4)10^{-3}$ emu/Ce at. Oe. From the inverse of χ_{cw} one can extract the Curie constant (Cc) which indicates a large but not fully developed Ce^{3+} magnetic moment (i.e., $\mu_{eff} = 2.32\mu_B$ per Ce atom). The paramagnetic temperature extrapolated from high-temperature ($T >$ 50 K) is notably small $\theta_P \leqslant 7$ K all along the concentration variation. This excludes any relevant influence of Kondo effect originated in local moments conduction-band hybridization.

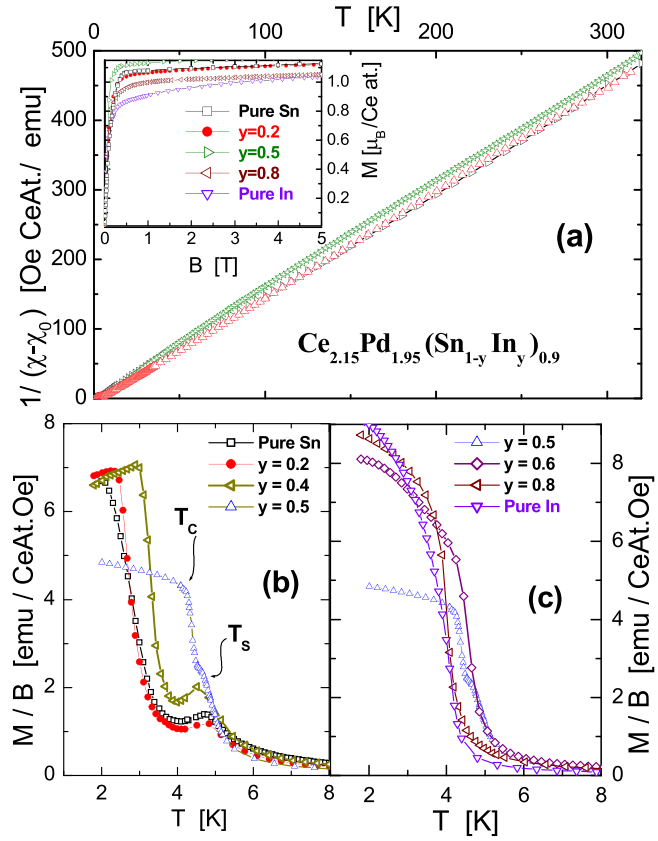

FIG. 2. (a) Inverse magnetic susceptibility from 1.8 K up to room temperature measured in a field $B = 1$ T. The inset: magnetization versus field up to 5 T, measured at 1.8 K. (b) Low-temperature susceptibility of Sn-rich alloys, measured with $B = 100$ Oe in a zero-field-cooling procedure. (c) The same for the In-rich concentrations. For comparison, sample $y = 0.5$ is included in both figures.

On the stoichiometric Sn limit, the sixfold-degenerated state established by Hund's rules for the $J = 5/2$ angular momentum of Ce atoms is split by the crystal electric-field (CEF) effect into three Kramer's doublets with the excited ones at $\Delta_1 \approx 65$ and $\Delta_2 \approx 230$ K [11]. A similar value ($\Delta_1 \approx 60$ K) was reported for the first excited doublet on the In-rich side [15]. This similarity indicates that no relevant modification of the CEF occurs along the Sn/In substitution and this guarantees that the low-temperature magnetic properties are governed by a pure doublet GS.

Magnetization $M(B)$ curves at $T = 1.8$ K are shown in the inset of Fig. 2(a). The saturation values slightly increase from $1.02\mu_B$ to $1.13\mu_B$ between pure Sn and In limits with a maximum value of $1.18\mu_B$ at $y \approx 0.5$.

In Figs. 2(b) and 1(c), detailed magnetic measurements around the transition temperatures are presented after being

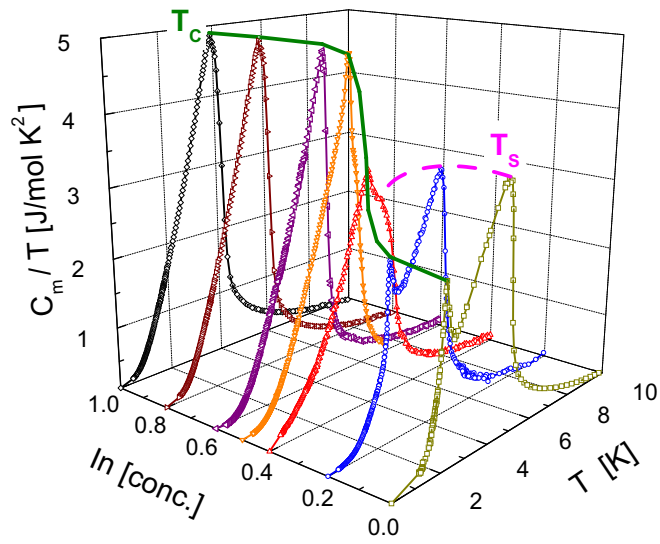

FIG. 3. Magnetic contribution to the specific heat of the measured alloys in a 3D representation. $T_C(y)$ indicates the FM transition (continuous curve), and $T_S(y < 0.5)$ indicates the boundary between paramagnetic and ShSu phases (dashed curve).

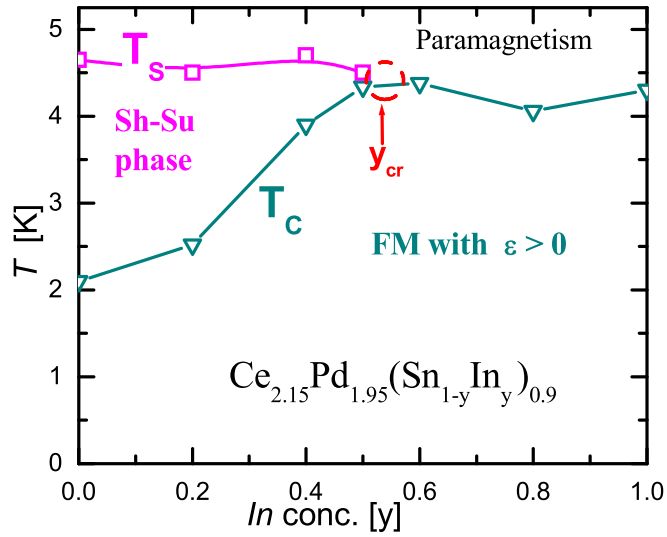

FIG. 4. Magnetic phase diagram showing the evolution of the Curie (T_C) and Shastry-Sutherland (T_S) transitions as a function of In increase.

normalized by magnetic-field M/B. These figures allow the comparison between different behaviors observed on both sides (Sn rich and In rich) of concentration and to recognize the magnetic nature of the observed transitions. As can be appreciated, the $0 \leqslant y \leqslant 0.5$ alloys show two transitions, one defined by an AFM maximum at $T = T_S$ followed a lower temperature by another with FM character at $T = T_C$, see Fig. 2(b). On the contrary, on the $0.5 \leqslant y \leqslant 1$ side [cf. Fig. 2(c)], only FM-type transitions are observed. Both $T_S(y)$ and $T_C(y)$ transitions join around a critical concentration $y_{cr} \approx 0.5$ with the $y = 0.5$ sample included in both figures for comparison.

C. Specific heat

In order to extract the magnetic contribution (C_m) to the measured specific-heat (C_P), the La_2Pd_2In compound was used as a reference [11] for the phonon subtraction: $C_m = C_P(T) - C(La_2Pd_2In)$. On the Sn-rich side, the two magnetic transitions observed in magnetic measurements presented in Fig. 2(b) are replicated in corresponding $C_m(T)/T$ jumps shown in Fig. 3. On the Sn-rich side, the specific-heat jump at $T_S(y)$ (dashed curve), the transition between the frustrated paramagnetic phase, and the ShSu one is of second-order type, whereas the FM transition (T_C) shows the characteristic of first-order type. However, above the critical concentration ($y_{cr} \approx 0.5$) at which the ShSu phase is suppressed, the only transition $T_C(y)$ becomes of second order, keeping the tail originated in the magnetic fluctuations arising above the transition.

As mentioned before, in stoichiometric Ce_2Pd_2Sn under a magnetic field [12], the ShSu phase is suppressed by increasing the temperature of the FM transition up to a critical field $B_{cr} \approx 1100$ Oe. A similar effect is observed by changing the electron concentration doping the Sn lattice with In because $T_C(y)$ increases from 2.1 K (at $y = 0$) up to the critical point at $T_{cr} = 4.15$ K and $y_{cr} \approx 0.5$, without any relevant change in $T_S(y)$. Notably, the strength of the C_m/T jump on the In-rich side $T_C(y > 0.5)$ is clearly larger than the one on the Sn side of $T_S(y < 0.5)$. This indicates that the transition at $T = T_S$ corresponds to an intermediate phase because it is related to Ce-Ce dimers formation. Thus, the change in entropy between paramagnetic and ShSu phases is $\Delta S_m(T_S) = R(\ln 2 - 1/2 \ln 3)$, only about 20% of the total entropy [11]. The remaining degrees of freedom condense into the FM-GS at $T < T_C$. Differently, the transitions in the $y \geqslant y_{cr}$ range involve all magnetic degrees of freedom, and the specific heat almost reaches the mean-field value predicted for a doublet GS.

III. DISCUSSION

A. Magnetic phase diagram and critical region

Based on magnetic and specific-heat results, the evolution of the Shastry-Sutherland (T_S) and Curie (T_C) transitions can be traced as a function of In increase. One can see that the ShSu phase, observed within the $T_C(y) \leqslant T \leqslant T_S(y)$ range forms up to slightly above 50% of In concentration, where $T_C(y)$ and $T_S(y)$ join into a tricritical point, see Fig. 4.

On the Sn-rich side, the characteristics of the ShSu phase recognized in Ce_2Pd_2Sn [11] can be clearly traced up to the sample with 40% of Sn substitution by In ($y = 0.4$). Although, at that concentration, both T_S and T_C transitions are observed as a structure within a unique broad anomaly in specific-heat measurements [see Fig. 5(a)], a more sensitive analysis through the $M(T)$ derivatives allows to better identify both approaching transitions. For such analysis, one can use the thermodynamic property of FM systems in which the internal magnetic energy $U_m \propto M^2$ and, therefore, $C_m \propto \delta M^2/\delta T$ [16] as shown in Fig. 5(a).

Another identification for a ShSu phase formation can be performed analyzing its suppression by a magnetic field in comparison with the same effect in stoichiometric Ce_2Pd_2Sn

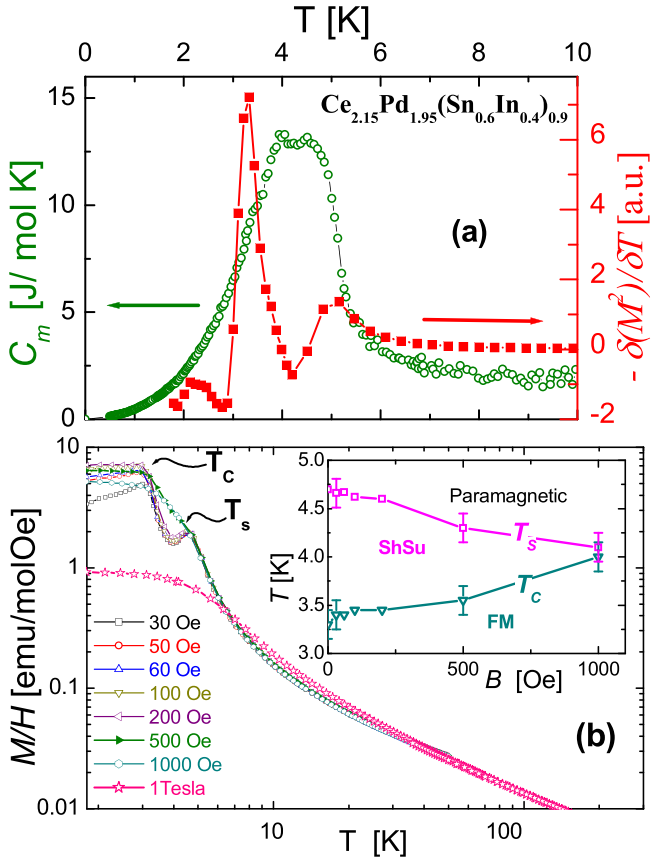

FIG. 5. (a) Comparison between specific-heat measurement (left axis) and magnetization derivative (right axis) for the $Ce_{2.15}Pd_{1.95}(Sn_{0.6}In_{0.4})_{0.9}$ alloy. (b) Progressive ShSu phase suppression by a magnetic field at 40% of In concentration in double logarithmic representation. The inset: phase diagram showing the evolution of T_C and T_S transitions as a function of applied field.

[12]. Shown in Fig. 5(b) is the $M/H(T, B)$ dependence of sample $y = 0.4$ with a detail of the $T_S(B)$ and $T_C(B)$ dependence in the magnetic phase diagram included in the inset. It can be seen that the collapse of the ShSu phase in that alloy occurs at $B_{cr}(y = 0.4) \approx 1000$ Oe, very close to the field intensity observed in the stoichiometric compound [12]. This suggests that the transitions at T_S does not change its nature despite the FM phase below T_C being strengthened by the magnetic field.

As mentioned above, the suppression of the ShSu phase by increasing In concentration occurs where the $T_S(y)$ and the $T_C(y)$ phase boundaries join, slightly above the 50% substitution. In Fig. 6, the specific-heat transitions of two neighboring concentrations $y = 0.5$ and 0.6 are compared making evident that the latter shows no structure around its maximum, such as that observed for $y = 0.5$. Coincidentally, there is practically no difference between respective entropies collected up to the transition. In the inset of that figure, a more detailed comparison is performed using respective magnetization derivatives as clearer evidence that the critical point lies between both concentrations. Notably, the first-order-type cusp in the $y = 0.5$ sample at $T_C \approx 4.3$ K and that at $T_S \approx 4.8$ K merge together at the next concentration $y = 0.6$.

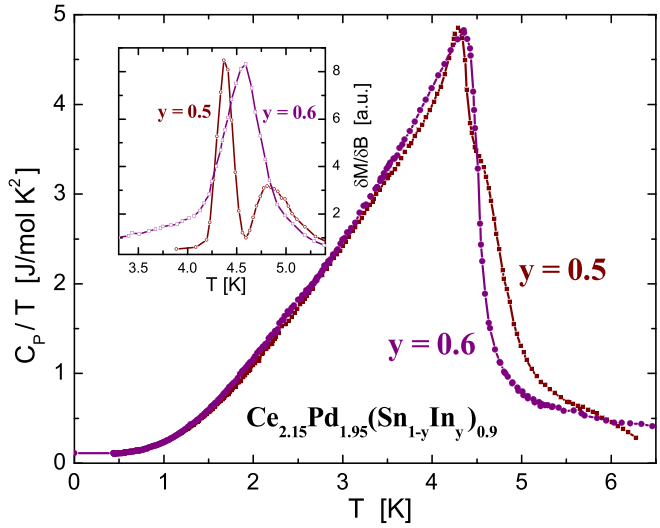

FIG. 6. Critical concentration determined by specific heat and, in the inset, by the magnetization derivatives of samples $y = 0.5$ and $y = 0.6$.

B. Physical behavior beyond the critical point

Between $y = 0.6$ and 1, the typical FM $M(T)$ dependence is observed according to the $M/H(T)$ results shown in Fig. 2(c), in agreement with the C_m/T_C jumps displayed in Fig. 3. Independent from this low-temperature behavior, samples $y = 0.6$ and 0.8 show an unexpected FM signal in the thermal dependence of its magnetic susceptibility arising at $T \leqslant 30$ K. This feature is weakly observed in $y = 0.6$ but better defined in $y = 0.8$ as presented in Fig. 7. This FM contribution was analyzed as a function of magnetic field at $T = 25$ K. In the inset of Fig. 7, one can appreciate the increase in this extra magnetization with field $\Delta M_{25\,K}(B)$ which saturates at $B \approx 0.3$ T with a quite small value of $\approx 5.4 \times 10^{-3}\mu_B$. Such an unexpected contribution cannot be explained by any foreign phase constituted by any combination of the four elements Ce-Pd-Sn-In. Therefore, it could be attributed

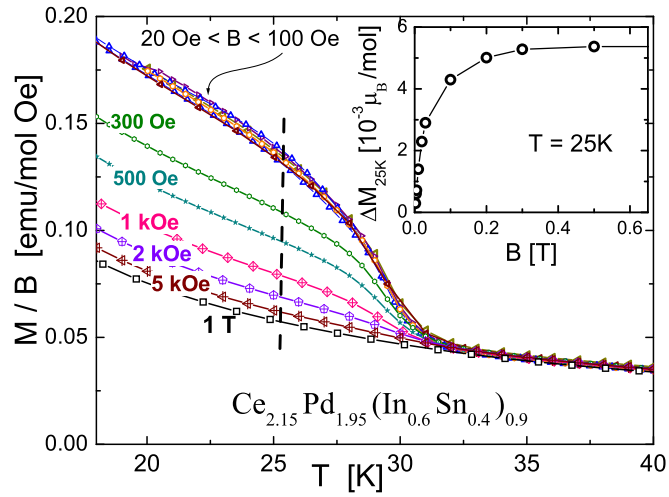

FIG. 7. Field dependence of the unexpected ferromagnetic contribution below ≈30 K tentatively attributed to spin-density waves formation. The inset: Magnetization increase upon the bulk magnetization at 25 K.

to intrinsic electron-band properties spin-density waves formation. Further transport and microscopic measurements are required to shed light into the actual nature and origin of this anomalous behavior.

IV. CONCLUSIONS

This paper demonstrates that, contrary to the Pd-rich AFM branch of the $Ce_2Pd_2(In_{1-x}Sn_x)$ solid solution, the Ce-rich FM one shows well-defined transitions with irrelevant atomic disorder produced by the Sn/In substitution. As a consequence, the upper $T_S(y)$ and the lower $T_C(y)$ boundaries of the ShSu phase can be clearly traced up to $y \approx 50\%$ of Sn substitution by In where a tricritical point is observed. The reduction of the electronic concentration driven by doping the $[5s^25p^2]$-Sn lattice with $[5s^25p^1]$-In atoms progressively weakens the stability of the ShSu phase as it is reflected in the monotonous growing of the FM phase-transition T_C.

The magnetic-field dependence was studied at the edge of the critical concentration: $y = 0.4$, showing similar weakening than that observed in the stoichiometric compound Ce_2Pd_2Sn, although only $1/2$ of intensity is required to suppress the ShSu phase.

Although Ce-rich content reduces atomic disorder effects allowing to extend the ShSu phase range, a further decrease in electronic concentration by Sn/In substitution definitively suppresses the possibility of dimers formation on which the simple square ShSu lattice builds up. Since this lattice forms within the Ce planes, one may expect that, on the In-rich side (i.e., $y > 0.5$), interplane interactions develop hand by hand with the increasing FM character of the Ce planes. This induces the system to behave as a 3D-FM above the critical concentration.

The unexpected observation of a FM signal at $T \leqslant 30$ K in the $y = 0.8$ sample cannot be attributed to the participant elements, and its weak saturation value induces to relate it to band magnetism originated in spin-density waves' formation. It is evident that complementary investigations are required to properly determine the nature and origin of this anomalous behavior.

[1] M. Lukachuk and R. Pöttgen, Intermetallic compounds with ordered U_3Si_2 or Zr_3Al_2 type structure-crystal chemistry, chemical bonding and physical properties, Z. Kristallogr. **218**, 767 (2003).

[2] D. Kaczorowski, P. Rogl, and K. Hiebl, In Magnetic behavior in a series of cerium ternary intermetallics: Ce_2T_2In (T=Ni, Cu, Rh, Pd, Pt, and Au), Phys. Rev. B **54**, 9891 (1996).

[3] S. K. Dhar, R. Settai, Y. ōnuki, A. Galatanu, Y. Haga, P. Manfrinetti, and M. Pani, Synthesis, crystal structure and magnetic properties of $Yb_8Ag_{18.5}Al_{47.5}$, Yb_2Pd_2Cd and $Yb_{1.35}Pd_2Cd_{0.65}$, J. Magn. Magn. Mater. **308**, 143 (2007).

[4] E. Bauer, G. Hilscher, H. Michor, C. Paul, Y. Aoki, H. Sato, D. Adroja, J.-G. Park, P. Bonville, C. Godart, J. Sereni, M. Giovannini, and A. Saccone, The magnetic instability of Yb_2Pd_2(In,Sn) in a non-Fermi liquid environment, J. Phys.: Condens. Matter **17**, S999 (2005).

[5] T. Muramatsu, T. Kanemasa, T. Kagayama, K. Shimizu, Y. Aoki, H. Sato, M. Giovannini, P. Bonville, V. Zlatic, T. Aviani, R. Khasanov, C. Rusu, A. Amato, K. Mydeen, M. Nicklas, H. Michor, and E. Bauer, Reentrant quantum criticality in Yb_2Pd_2Sn, Phys. Rev. B **83**, 180404(R) (2011).

[6] F. Fourgeot, P. Gravereau, B. Chevalier, L. Fournés, and J. Etourneau, Effect of the chemical composition on the structural properties of the antiferromagnetic ternary stannides $Ce_2Pd_{2+x}Sn_x$ $(0.04(3) \leqslant x \leqslant 0.21(4))$, J. Alloys Comput. **238**, 102 (1996).

[7] B. S. Shastry and B. Sutherland, Exact ground state of quantum mechanical antiferromagnet, Physica **108B**, 1069 (1981).

[8] H. Kageyama, K. Yoshimura, R. Stern, N. V. Mushnikov, K. Onizuka, M. Kato, K. Kosuge, C. P. Slichter, T. Goto, and Y. Ueda, Exact Dimer Ground State and Quantized Magnetization Plateaus in the Two-Dimensional Spin System $SrCu_2(BO_3)_2$, Phys. Rev. Lett. **82**, 3168 (1999).

[9] M. S. Kim and M. C. Aronson, Heavy fermion compounds on the geometrically frustrated Shastry-Sutherland lattice, J. Phys.: Condens. Matter **23**, 164204 (2011).

[10] L. S. Wu, W. J. Gannon, I. A. Zaliznyak, A. M. Tsvelik, M. Brockmann, J.-S. Caux, M. S. Kim, Y. Qiu, J. R. D. Copley, G. Ehlers, A. Podlesnyak, and M. C. Aronson, Orbital-exchange and fractional quantum number excitations in an f-electron metal, Yb_2Pt_2Pb, Science **352**, 1206 (2016).

[11] J. G. Sereni, M. G-Berisso, A. Braghta, G. Schmerber, and J. P. Kappler, Unstable Shastry-Sutherland phase in Ce_2Pd_2Sn, Phys. Rev. B **80**, 024428 (2009).

[12] J. G. Sereni, M. Gomez Berisso, G. Schmerber, and J. P. Kappler, Suppression of the Shastry-Sutherland phase in Ce_2Pd_2Sn at a field-induced critical point, Phys. Rev. B **81**, 184429 (2010).

[13] J. G. Sereni, J. Roberts, F. Gastaldo, M. G-Berisso, and M. Giovannin, Shastry-Sutherland phase formation in magnetically frustrated $Ce_2Pd_2In_{1-x}Sn_x$ alloys, Mater. Today Proc. **14**, 80 (2019).

[14] M. Giovannini, H. Michor, E. Bauer, and G. Hilscher, P. Rogl, T. Bonelli, F. Fauth, P. Fischer, T. Herrmannsdo, L. Keller, W. Sikora, A. Saccone, and R. Ferro, Effect of nonstoichiometry on the transition from ferromagnetism to antiferromagnetism in the ternary Indides $Ce_{1.95}Pd_{2+2x}In_{1-x}$ and $Ce_{2+x}Pd_{1.85}In_{1-x}$, Phys. Rev. B **61**, 4044 (2000).

[15] J. G. Sereni, M. Giovannini, M. Gomez Berisso, and A. Saccone, Electron concentration effects on the Shastry-Sutherland phase stability in $Ce_{2-x}Pd_{2+y}In_{1-z}$ solid solutions, Phys. Rev. B **83**, 064419 (2011).

[16] K. P. Belov, *Magnetic Transitions* (Consultants Bureau, New York, 1961), Chap. 1, p. 61.